


Realization of Strong Coupling between Deterministic Single-Atom Arrays and a High-Finesse Miniature Optical Cavity

Yanxin Liu^{✉,*}, Zhihui Wang,^{*} Pengfei Yang, Qinxia Wang, Qing Fan, Shijun Guan,
Gang Li^{✉,†}, Pengfei Zhang,[‡] and Tiancai Zhang[§]

*State Key Laboratory of Quantum Optics and Quantum Optics Devices, and Institute of Opto-Electronics,
Shanxi University, Taiyuan 030006, China
and Collaborative Innovation Center of Extreme Optics, Shanxi University, Taiyuan 030006, China*

 (Received 15 July 2022; revised 12 March 2023; accepted 11 April 2023; published 28 April 2023)

We experimentally demonstrate strong coupling between a one-dimensional (1D) single-atom array and a high-finesse miniature cavity. The atom array is obtained by loading single atoms into a 1D optical tweezer array with dimensions of 1×11 . Therefore, a deterministic number of atoms is obtained, and the atom number is determined by imaging the atom array on a CCD camera in real time. By precisely controlling the position and spacing of the atom array in the high finesse Fabry-Perot cavity, all the atoms in the array are strongly coupled to the cavity simultaneously. The vacuum Rabi splitting spectra are discriminated for deterministic atom numbers from 1 to 8, and the \sqrt{N} dependence of the collective enhancement of the coupling strength on atom number N is validated at the single-atom level.

DOI: [10.1103/PhysRevLett.130.173601](https://doi.org/10.1103/PhysRevLett.130.173601)

A strongly coupled cavity quantum electrodynamics (QED) system is a basic physical system for studying light-matter interactions [1], which not only is a test bed for studying fundamental physics but also provides powerful quantum resources for quantum information [2–6]. Matured through single-atom control in the small cavity mode, vacuum Rabi splitting of a single atom has been observed [7–9], which has provided great significance in quantum physics. As promising platforms to realize quantum networks [10], optical cavity QED systems have attracted intense interest. Research has been mainly focused on the interaction between single atoms and single photons. Many new quantum technologies and devices, e.g., single-photon sources and blockades [11–17], quantum interfaces [18,19], quantum logic gates [20–23], quantum measurements [24–29], and quantum routers [30–34], have been developed and investigated. Significantly, the demonstration of an elementary quantum network [35] between two nodes with an individual atom in each cavity has brought a great leap forward for quantum networks.

The multiatom cavity QED system, in which individual atoms can be discriminated and controlled, would be more interesting for both fundamental physics and applications. First, the cavity photon-mediated interactions between different atoms enrich the dynamics and complexity of the coupling diagrams for many-body physics research [36–38]. Moreover, in the context of the recent progress in programmable arrays of atoms in quantum simulations and quantum computations [39–44], the development of a multiqubit module with optical links, which can process quantum information locally and interface qubits between

atoms and photons, brings new perspectives for quantum networks and distributed quantum computation [45].

However, building such a multiatom cavity QED system is quite challenging because of the stringent requirement on the position control of every atom to obtain steady and uniform strong coupling to a tiny cavity mode for each atom. To date, only two neutral atoms have been successfully controlled in the same mode of a Fabry-Perot (FP) or nanophotonic cavity [45–48]. A cavity QED system with one-dimensional (1D) atom arrays transversely integrated with a high finesse FP cavity has also been recently presented [49–51]. However, the atoms are not uniformly coupled to the cavity mode. A system of 5 ions coupled to an FP cavity has also been demonstrated [52], but not in the strong coupling regime. In this Letter, we report strong coupling between 1D atom arrays and a miniature FP cavity. The atom arrays are engineered to couple to the cavity simultaneously with a uniform coupling strength. Strong coupling of up to 8 atoms of an 11-tweezer array is demonstrated. Vacuum Rabi splitting can be discriminated from 1 to 8 atoms individually, and the \sqrt{N} scaling of the collective enhancement of the coupling strength with atom number N is validated for a deterministic number of atoms.

The experimental setup is illustrated in Fig. 1(a). The core of the setup is a miniature optical FP cavity [a picture can be found in Supplemental Material (SM)] [53], which is composed of two high-reflectively coated mirrors with a curvature radius of 100 mm. The mirrors have transmittances of 4.9 and 84.9 ppm at 852 nm. The length of the cavity is fixed at 1.27 mm to accommodate the atom array while maintaining strong coupling for individual atoms. The waist of the TEM_{00} mode and finesse of the

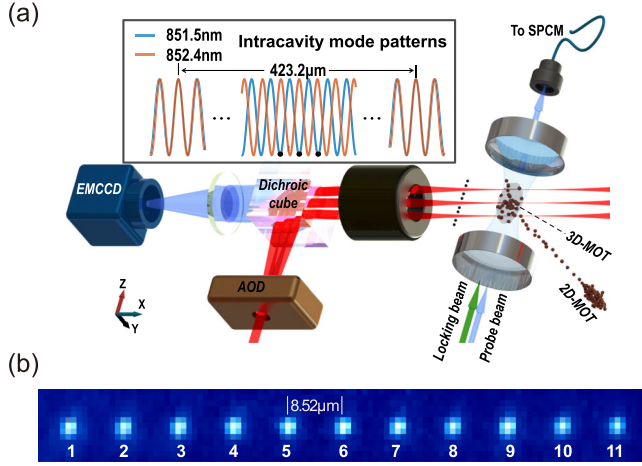


FIG. 1. Scheme of the experiment. (a) Sketch of the essential part of the experimental setup. The FP cavity is stabilized by an 851.5-nm locking beam, and another weak 852-nm probe beam (the corresponding intracavity mean photon number $\langle n \rangle = 0.1$) is used to measure the spectrum. Inset: an illustration of the mode patterns of the lattice (blue) and 852-nm field (red). (b) Image of single atom arrays obtained by superimposing approximately 500 loading trials. The exposure time was set as 40 ms for every trial.

cavity are $46 \mu\text{m}$ and 5.7×10^4 , respectively. Thus, the cavity QED parameters for individual cesium atoms in our system are $(g_0, \kappa, \gamma) = 2\pi \times (3.2, 1.0, 2.6)$ MHz, where g_0 denotes the theoretical maximum coupling strength between a cesium atom (for transition $|g\rangle \equiv 6S_{1/2}|F=4, m_F=4\rangle \leftrightarrow |e\rangle \equiv 6P_{3/2}|F=5, m_F=5\rangle$) and the cavity TEM₀₀ mode. κ and γ are the decay rates for the cavity and atom, respectively. The cooperative coefficient is $C = g_0^2/2\kappa\gamma = 1.9$, which means that our system is a strongly coupled cavity QED system for a single atom when the position can be controlled precisely at the antinode of the cavity standing-wave mode.

The details of the experimental apparatus, including the optical cavity, the vacuum system, and the cavity locking scheme, can be found in SM [53]. The whole cavity system is placed inside a high-vacuum glass cell with inner dimensions of $20 \text{ mm} \times 25 \text{ mm}$ on the cross section. The length of the cavity is actively stabilized to the cesium transition line $|g\rangle \leftrightarrow |e\rangle$ (the resonant wavelength is approximately 852.356 nm) by an auxiliary locking laser at 851.5 nm (three free spectral ranges off the atomic transition), whose frequency has been locked to the cesium transition line via a transfer cavity. The locking laser also forms a lattice with positive potentials along the cavity axis. Because of the relatively long cavity length, a small magneto-optical trap (MOT) can be built directly inside the FP cavity to accumulate the atoms emitted from the first-stage two-dimensional MOT. The atomic ensemble has a diameter of $150 \mu\text{m}$ and an atom number of approximately 10^5 . The temperature is approximately $15 \mu\text{K}$ after polarization gradient cooling.

The optical tweezer array is generated by strongly focusing a 1D laser beam array with dimensions of 1×11 by a homemade high-numerical-aperture objective with $NA = 0.4$ and focal length $f = 28.8 \text{ mm}$ [58]. The laser beam array comes from the diffraction of an acousto-optic deflector (AOD, DTSX, AA Opto Electronic) driven by a multitone radio frequency (rf) signal. Every tweezer has a waist radius of $1.81 \mu\text{m}$, which ensures that only a single atom is loaded by the light-assisted collision process [59]. The tweezer array is projected into the cavity transversely from the outside of the vacuum glass cell and the orientation is along the cavity axis (Z axis). The optical tweezers load single atoms directly from the precooled cesium atom ensemble. The fluorescence of the loaded single atoms is collected by the same objective, separated from the trapping beam by a dichroic beam splitter cube, and eventually imaged on an electron-multiplying CCD (EMCCD) camera. Figure 1(b) shows an average picture of the single atoms trapped by the tweezer array.

Figure 2(a) shows a typical histogram of the fluorescence from one of the tweezers recorded by the EMCCD camera. The bimodal structure of the count distribution indicates that each time, only one atom is loaded into one tweezer, and the loading probability is approximately 57%. The average lifetime for the trapped individual atom is measured to be approximately $4.8(1) \text{ s}$ [as shown in Fig. 2(b)] when the tweezer overlaps with the intracavity lattice. The lifetime is limited by the heating due to the variance of the position overlap between the optical tweezer and the intracavity lattice. Figure 2(c) shows the atom number distribution in all 11 optical tweezers. From the single-atom loading probability (57%), we expect the average atom number for all 11 tweezers to be approximately 6.3. However, we only obtain a value of 5 from Fig. 2(c). The reason is that several tweezers on the edge do not exactly overlap with the atomic ensemble in the measurement. If all the tweezers overlap well with the atomic ensemble, then the average atom number could reach the expected result.

The challenge of the experiment is to control the position of every atom to reach maximum and steady coupling to the cavity. To obtain this condition, the position of each tweezer should not only exactly overlap with an antinode of the cavity standing-wave mode in the Z direction but also be in the center of the mode profile in both the X and Y directions. However, since the size of the optical tweezer is much larger than the structure of the standing wave, the atom cannot be confined around the small antinode region by the optical tweezer alone. With the aid of the blue-detuned lattices induced by the 851.5-nm locking laser the problem can be resolved.

When the blue lattice is taken into account, the atom trapped in the tweezer will be pushed to a node of the lattice. The node of the lattice overlaps perfectly with the antinode of the cavity mode at the center of the 852-nm

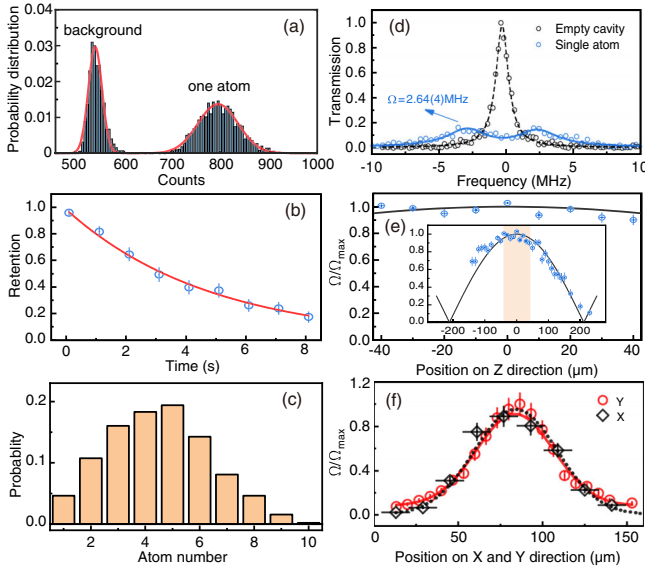


FIG. 2. (a) Typical histogram of the electron counts of the fluorescence from the No. 6 optical tweezer in Fig. 1(b) on the EMCCD camera for 5000 trials of atom loading. The red line is the fitting with a bimodal Gaussian function. (b) Atom retention versus atom holding time. The exponential fitting gives a characteristic atom lifetime of 4.8(1) s. (c) Probability of the number of single atoms loaded into all 11 optical tweezers. The probabilities are counted for 500 trials of atom loading, giving an average atom number of approximately 5. (d) Typical spectra during optimization. The light blue circles represent the experimental data with one tweezer on. The coupling strength Ω is determined by fitting with Eq. (1). The spectrum of the empty cavity is also shown for comparison (black circles). (e) Optimization of the position of the atom on the Z axis. The main figure shows the variance of the coupling strength in the position range from -42.6 to 42.6 μm (shaded area of the inset figure), in which the optical tweezer arrays are placed. The inset shows the variance of coupling strength in a larger range. The black solid line is the theoretical coupling strength between the cavity and atom when the atom is trapped in different nodes of the intracavity lattice. The light blue circles are the measured atom-cavity coupling versus the atom position with only one tweezer on. (f) Dependence of the atom-cavity coupling on the X and Y axis positions. All eleven tweezers are used for these measurements. The fittings by Gaussian functions give mode waists of 48.0(2.8) and 45.7(2.8) μm along the X and Y axes, respectively.

mode where the coupling between the atom and the cavity is maximum. The node of the lattice will gradually displace from the antinode of the 852-nm mode and totally mismatch with each other at the offset position with a distance of 216.6 μm to the cavity center, where the atom decouples to the cavity. The overlap repeats for every 423.2 μm along the Z direction. The solid line in Fig. 2(e) presents the theoretical prediction of the coupling strength of the atom when it is trapped in different sites of the lattice along the Z direction.

To verify the coupling pattern of the atom, only one tweezer is used to load the atom and test the coupling.

The tweezer is switched on by driving the AOD with a single tone rf signal of 79.8 MHz. The position of the tweezer trap in the Z direction can be scanned by either a motorized stage or the rf driving frequency applied to the AOD. Here, it is scanned step by step by the motorized stage. At every scanned spatial point, a single atom is loaded into the tweezer and the atom-cavity coupling strength is checked by measuring the vacuum Rabi splitting spectrum. A typical spectrum is shown as the light blue data points in Fig. 2(d). The coupling strength Ω can be obtained by fitting the data with the theoretical transmission spectrum [53]

$$T = \frac{\kappa^2(\gamma^2 + \Delta_{pa}^2)}{(\Omega^2 - \Delta_{pa}^2 + \Delta_{ca}\Delta_{pa} + \gamma\kappa)^2 + (\kappa\Delta_{pa} + \gamma\Delta_{pa} - \gamma\Delta_{ca})^2}, \quad (1)$$

where Δ_{ca} (Δ_{pa}) is the frequency detuning between the cavity (probe) and atom. Ω is the coupling strength, which equals g for a single atom. Δ_{ca} can also be determined by fitting. The relative coupling strength $\Omega/\Omega_{\text{max}}$, where Ω_{max} is the maximum in one scan trial, versus the position on the Z axis is shown as the blue circles in Fig. 2(e), which agrees well with the theoretical prediction from the overlap between the blue lattice and 852-nm cavity mode.

Thus, maximum and steady coupling can be naturally achieved as long as the 11 tweezers are placed around the center of the cavity where the node of the lattice and the antinode of the 852-nm mode coincide well in space [as shown in the inset of Fig. 1(a)]. The 11 tweezers are switched on with the center rf frequency fixed at 79.8 MHz. The distance between the neighboring tweezers is set as 8.52 μm by setting the spacing of the multitone rf frequency as 1.16 MHz. The spatial offset of the tweezers at the edge is ± 42.6 μm to the cavity center. The coupling of the atom in the edge tweezer is 95% of the one in the center in theory. The theoretical variance of the coupling for all 11 atoms in the tweezer array is only $\pm 2.5\%$. From the data measured in Fig. 2(e) we obtain that the variance of the measured coupling strength is within $\pm 4\%$.

After the Z positions of the atomic array have been optimized at the maximum coupling spots, the positions in the X and Y directions are also scanned with all eleven tweezers on. The measured coupling coefficients versus the X and Y positions are displayed in Fig. 2(f), where the results follow a Gaussian mode profile well. The fitting of the results by Gaussian functions gives mode waists in the X and Y directions of 48.0(2.8) and 45.7(1.7) μm , respectively, which are in good agreement with those calculated from the geometry of the FP cavity. Therefore, by setting the positions in the X and Y directions to the maximum coupling spots, we can eventually optimize and realize strong coupling between deterministic atom arrays and the FP cavity.

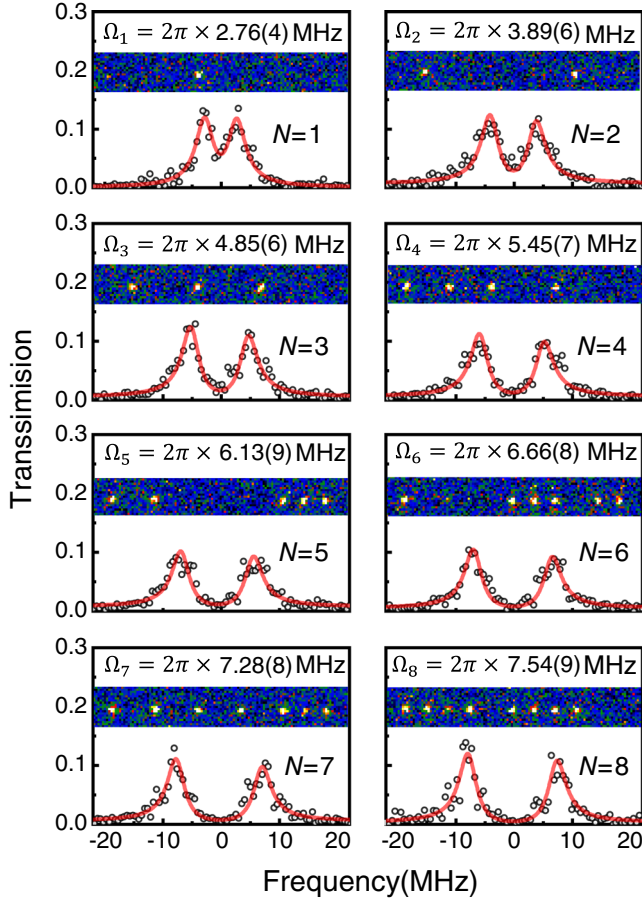


FIG. 3. Vacuum Rabi splitting with a deterministic atom number from $N = 1$ to $N = 8$. The single shot images of the trapped atoms are shown as the inset picture, which are used to precisely count the atom number. The experimental data (black circles) are fitted (red lines) by Eq. (1) to determine Ω_N .

In principle, our cavity QED system can realize strong coupling between the FP cavity and atoms with a deterministic number less than 11. Here, we demonstrate coupling between the cavity and atom arrays with atom numbers from 1 to 8. The measured vacuum Rabi spectra in the transmission and images of the atom arrays are depicted in Fig. 3. The atom number is exactly determined from the EMCCD image and the coupling strength Ω is extracted by fitting with Eq. (1). The measured vacuum Rabi splitting of a single atom is $2g = 2\pi \times 5.52(8)$ MHz, which is approximately 87% of the maximum theoretical value of $2\pi \times 6.32$ MHz. The difference mainly comes from the imperfect state initialization efficiency ($\sim 91\%$). The average due to residual motion of the atom will also produce a smaller g . The unequal height of the two normal splitting peaks in Fig. 3 mainly comes from the uneven Δ_{ca} in different tweezers. Since we leave all the tweezers on with a shallow trap depth (~ 0.1 mK) during the measurement, the light shifts of atoms in different tweezers are uneven due to the small variance in the trap shapes and intensities. The Δ_{ca} values extracted from the data

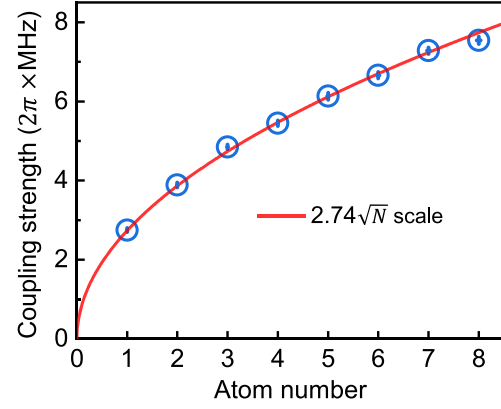


FIG. 4. Dependence of the collective coupling strength on the atom number. The solid red line is the theoretical result for the collective enhancement relation $\Omega_N = g\sqrt{N}$ with the measured single atom coupling strength $g = 2\pi \times 2.74$ MHz.

fitting are within the range of 0–0.4 MHz for all the subfigures.

The extracted vacuum Rabi splitting Ω_N versus atom number N is displayed in Fig. 4. The single-atom coupling strength g can also be deduced from Ω_N by $g = \Omega_N/\sqrt{N}$. We obtained eight values of g corresponding to atom numbers from 1 to 8. The variance in g is within $\pm 2\%$ of the average value $2\pi \times 2.74$ MHz. The single-atom coupling strength can also be obtained by fitting the data with $g' = \Omega_N/\sqrt{N}$, which gives $g' = 2\pi \times 2.73(1)$ MHz, and it is almost the same as the averaged value.

Collective enhancement of light-matter interactions by using multiple single atoms is a basic principle in quantum physics. The dependence of the collective enhancement on the atom number has been proven through Rydberg excitation of atoms [60,61] and single qubits in superconducting circuits [62]. Here, this fundamental relation can be tested by using deterministic atom numbers with discrimination at the real single-atom level in our cavity QED system. As displayed in Fig. 4, the theoretical collective enhancement relation $\Omega_N = g\sqrt{N}$ is shown as the red line with the single-atom coupling strength $g = 2\pi \times 2.74$ MHz. We see that the scaling of experimental data with the atom number agrees very well with the theory, which validates the principle of collective enhancement.

In summary, we have developed a new cavity QED system in which well-controlled 1D atom arrays are strongly coupled to a miniature FP cavity. Vacuum Rabi splittings with a deterministic number of atoms are observed; thus, the principle of collective enhancement of light-matter interactions with multiple atoms is experimentally tested and validated with single atoms. The system provides a versatile platform to study light-matter interactions, quantum networks with nodes containing multiple atomic qubits [63], and many-body physics with interactions mediated by photons [36–38,64].

This work was supported by the National Key Research and Development Program of China (Grants No. 2021YFA1402002 and No. 2017YFA0304502), the National Natural Science Foundation of China (Grants No. U21A6006, No. U21A20433, No. 11974223, No. 11974225, No. 12104277, and No. 12104278), and the Fund for Shanxi 1331 Project Key Subjects Construction.

*These authors contributed equally to this work.

†gangli@sxu.edu.cn

‡zhangpengfei@sxu.edu.cn

§tczhang@sxu.edu.cn

- [1] S. M. Dutra, *Cavity Quantum Electrodynamics* (John Wiley & Sons, Ltd, New York, 2004).
- [2] J. M. Raimond, M. Brune, and S. Haroche, Manipulating quantum entanglement with atoms and photons in a cavity, *Rev. Mod. Phys.* **73**, 565 (2001).
- [3] S. Haroche, Nobel lecture: Controlling photons in a box and exploring the quantum to classical boundary, *Rev. Mod. Phys.* **85**, 1083 (2013).
- [4] A. Reiserer and G. Rempe, Cavity-based quantum networks with single atoms and optical photons, *Rev. Mod. Phys.* **87**, 1379 (2015).
- [5] A. Blais, A. L. Grimsmo, S. M. Girvin, and A. Wallraff, Circuit quantum electrodynamics, *Rev. Mod. Phys.* **93**, 025005 (2021).
- [6] H. Ritsch, P. Domokos, F. Brennecke, and T. Esslinger, Cold atoms in cavity-generated dynamical optical potentials, *Rev. Mod. Phys.* **85**, 553 (2013).
- [7] R. J. Thompson, G. Rempe, and H. J. Kimble, Observation of Normal-Mode Splitting for an Atom in an Optical Cavity, *Phys. Rev. Lett.* **68**, 1132 (1992).
- [8] A. Boca, R. Miller, K. M. Birnbaum, A. D. Boozer, J. McKeever, and H. J. Kimble, Observation of the Vacuum Rabi Spectrum for One Trapped Atom, *Phys. Rev. Lett.* **93**, 233603 (2004).
- [9] P. Maunz, T. Puppe, I. Schuster, N. Syassen, P. W. H. Pinkse, and G. Rempe, Normal-Mode Spectroscopy of a Single-Bound-Atom-Cavity System, *Phys. Rev. Lett.* **94**, 033002 (2005).
- [10] H. J. Kimble, The quantum internet, *Nature (London)* **453**, 1023 (2008).
- [11] J. McKeever, A. Boca, A. D. Boozer, J. R. Buck, and H. J. Kimble, Experimental realization of a one-atom laser in the regime of strong coupling, *Nature (London)* **425**, 268 (2003).
- [12] J. McKeever, A. Boca, A. D. Boozer, R. Miller, J. R. Buck, A. Kuzmich, and H. J. Kimble, Deterministic generation of single photons from one atom trapped in a cavity, *Science* **303**, 1992 (2004).
- [13] A. Kuhn, M. Hennrich, and G. Rempe, Deterministic Single-Photon Source for Distributed Quantum Networking, *Phys. Rev. Lett.* **89**, 067901 (2002).
- [14] O. Morin, M. Körber, S. Langenfeld, and G. Rempe, Deterministic Shaping and Reshaping of Single-Photon Temporal Wave Functions, *Phys. Rev. Lett.* **123**, 133602 (2019).
- [15] K. M. Birnbaum, A. Boca, R. Miller, A. D. Boozer, T. E. Northup, and H. J. Kimble, Photon blockade in an optical cavity with one trapped atom, *Nature (London)* **436**, 87 (2005).
- [16] S. Rosenblum, O. Bechler, I. Shomroni, Y. Lovsky, G. Guendelman, and B. Dayan, Extraction of a single photon from an optical pulse, *Nat. Photonics* **10**, 19 (2016).
- [17] C. Hamsen, K. N. Tolazzi, T. Wilk, and G. Rempe, Two-Photon Blockade in an Atom-Driven Cavity QED System, *Phys. Rev. Lett.* **118**, 133604 (2017).
- [18] T. Wilk, S. C. Webster, A. Kuhn, and G. Rempe, Single-atom single-photon quantum interface, *Science* **317**, 488 (2007).
- [19] J. Schupp, V. Krcmarsky, V. Krutyanskiy, M. Meraner, T. E. Northup, and B. P. Lanyon, Interface between trapped-ion qubits and traveling photons with close-to-optimal efficiency, *PRX Quantum* **2**, 020331 (2021).
- [20] A. Reiserer, N. Kalb, G. Rempe, and S. Ritter, A quantum gate between a flying optical photon and a single trapped atom, *Nature (London)* **508**, 237 (2014).
- [21] B. Hacker, S. Welte, G. Rempe, and S. Ritter, A photon quantum gate based on a single atom in an optical resonator, *Nature (London)* **536**, 193 (2016).
- [22] O. Bechler, A. Borne, S. Rosenblum, G. Guendelman, O. E. Mor, M. Netser, T. Ohana, Z. Aqua, N. Drucker, R. Finkelstein, Y. Lovsky, R. J. Bruch, D. Gurovich, E. Shafir, and B. Dayan, A passive photon-atom qubit swap operation, *Nat. Phys.* **14**, 996 (2018).
- [23] S. Daiss, S. Langenfeld, S. Welte, E. Distante, P. Thomas, L. Hartung, O. Morin, and G. Rempe, A quantum-logic gate between distant quantum-network modules, *Science* **371**, 614 (2021).
- [24] J. Volz, R. Gehr, G. Dubois, J. Esteve, and J. Reichel, Measurement of the internal state of a single atom without energy exchange, *Nature (London)* **475**, 210 (2011).
- [25] A. Reiserer, S. Ritter, and G. Rempe, Nondestructive detection of an optical photon, *Science* **342**, 1349 (2013).
- [26] L. M. Duan and H. J. Kimble, Scalable Photonic Quantum Computation through Cavity-Assisted Interactions, *Phys. Rev. Lett.* **92**, 127902 (2004).
- [27] D. Niemietz, P. Farrera, S. Langenfeld, and G. Rempe, Nondestructive detection of photonic qubits, *Nature (London)* **591**, 570 (2021).
- [28] S. Welte, P. Thomas, L. Hartung, S. Daiss, S. Langenfeld, O. Morin, G. Rempe, and E. Distante, A nondestructive Bell-state measurement on two distant atomic qubits, *Nat. Photonics* **15**, 504 (2021).
- [29] E. Distante, S. Daiss, S. Langenfeld, L. Hartung, P. Thomas, O. Morin, G. Rempe, and S. Welte, Detecting an Itinerant Optical Photon Twice without Destroying It, *Phys. Rev. Lett.* **126**, 253603 (2021).
- [30] I. Shomroni, S. Rosenblum, Y. Lovsky, O. Bechler, G. Guendelman, and B. Dayan, All-optical routing of single photons by a one-atom switch controlled by a single photon, *Science* **345**, 903 (2014).
- [31] M. Scheucher, A. Hilico, E. Will, J. Volz, and A. Rauschenbeutel, Quantum optical circulator controlled by a single chirally coupled atom, *Science* **354**, 1577 (2016).
- [32] B. Dayan, A. Parkins, T. Aoki, E. P. Ostby, K. J. Vahala, and H. J. Kimble, A photon turnstile dynamically regulated by one atom, *Science* **319**, 1062 (2008).

- [33] A. Kubanek, A. Ourjoumtsev, I. Schuster, M. Koch, P. W. H. Pinkse, K. Murr, and G. Rempe, Two-Photon Gateway in One-Atom Cavity Quantum Electrodynamics, *Phys. Rev. Lett.* **101**, 203602 (2008).
- [34] T. Aoki, A. S. Parkins, D. J. Alton, C. A. Regal, B. Dayan, E. Ostby, K. J. Vahala, and H. J. Kimble, Efficient Routing of Single Photons by One Atom and a Microtoroidal Cavity, *Phys. Rev. Lett.* **102**, 083601 (2009).
- [35] S. Ritter, C. Nölleke, C. Hahn, A. Reiserer, A. Neuzner, M. Uphoff, M. Mücke, E. Figueroa, J. Bochmann, and G. Rempe, An elementary quantum network of single atoms in optical cavities, *Nature (London)* **484**, 195 (2012).
- [36] E. J. Davis, G. Bentsen, L. Homeier, T. Li, and M. H. Schleier-Smith, Photon-Mediated Spin-Exchange Dynamics of Spin-1 Atoms, *Phys. Rev. Lett.* **122**, 010405 (2019).
- [37] J. Muniz, D. Barberena, R. J. Lewis-Swan, D. J. Young, J. R. K. Cline, A. M. Rey, and J. K. Thompson, Exploring dynamical phase transitions with cold atoms in an optical cavity, *Nature (London)* **580**, 602 (2020).
- [38] A. Periwal, E. S. Cooper, P. Kunkel, J. F. Wienand, E. J. Davis, and M. Schleier-Smith, Programmable interactions and emergent geometry in an array of atom clouds, *Nature (London)* **600**, 630 (2021).
- [39] M. Saffman, T. G. Walker, and K. Mølmer, Quantum information with Rydberg atoms, *Rev. Mod. Phys.* **82**, 2313 (2010).
- [40] S. Ebadi, T. T. Wang, H. Levine, A. Keesling, G. Semeghini, A. Omran, D. Bluvstein, R. Samajdar, H. Pichler, W. W. Ho, S. Choi, S. Sachdev, M. Greiner, V. Vuletić, and M. D. Lukin, Quantum phases of matter on a 256-atom programmable quantum simulator, *Nature (London)* **595**, 227 (2021).
- [41] P. Scholl, M. Schuler, H. J. Williams, A. A. Eberharter, D. Barredo, K. N. Schymik, V. Lienhard, L. P. Henry, T. C. Lang, T. Lahaye, A. M. Läuchli, and A. Browaeys, Quantum simulation of 2D antiferromagnets with hundreds of Rydberg atoms, *Nature (London)* **595**, 233 (2021).
- [42] I. S. Madjarov, J. P. Covey, A. L. Shaw, J. Choi, A. Kale, A. Cooper, H. Pichler, V. Schkolnik, J. R. Williams, and M. Endres, High-fidelity entanglement and detection of alkaline-earth Rydberg atoms, *Nat. Phys.* **16**, 857 (2020).
- [43] T. M. Graham, Y. Song, J. A. Scott, C. Poole, L. Phuttitarn, K. Jooya, P. Eichler, X. Jiang, A. A. Marra, B. Grinkemeyer, M. Kwon, M. Ebert, J. Cherek, M. Lichtman, M. Gillette, J. P. Gilbert, D. N. Bowman, T. Ballance, C. Campbell, E. D. Dahl, O. Crawford, N. Blunt, B. R. T. W. Noel, and M. Saffman, Multi-qubit entanglement and algorithms on a neutral-atom quantum computer, *Nature (London)* **604**, 457 (2022).
- [44] D. Bluvstein, H. Levine, G. Semeghini, T. T. Wang, S. Ebadi, M. Kalinowski, A. Keesling, N. Maskara, H. Pichler, M. Greiner, V. Vuletić, and M. D. Lukin, A quantum processor based on coherent transport of entangled atom arrays, *Nature (London)* **604**, 451 (2022).
- [45] T. Dordević, P. Samutpraphoot, P. L. Ocola, H. Bernien, B. Grinkemeyer, I. Dimitrova, V. Vuletić, and M. D. Lukin, Entanglement transport and a nanophotonic interface for atoms in optical tweezers, *Science* **373**, 1511 (2021).
- [46] B. Casabone, A. Stute, K. Friebe, B. Brandstätter, K. Schüppert, R. Blatt, and T. E. Northup, Heralded Entanglement of Two Ions in an Optical Cavity, *Phys. Rev. Lett.* **111**, 100505 (2013).
- [47] S. Welte, B. Hacker, S. Daiss, S. Ritter, and G. Rempe, Cavity Carving of Atomic Bell States, *Phys. Rev. Lett.* **118**, 210503 (2017).
- [48] R. Reimann, W. Alt, T. Kampschulte, T. Macha, L. Ratschbacher, N. Thau, S. Yoon, and D. Meschede, Cavity-Modified Collective Rayleigh Scattering of Two Atoms, *Phys. Rev. Lett.* **114**, 023601 (2015).
- [49] E. Deist, J. A. Gerber, Y.-H. Lu, J. Zeiher, and D. M. Stamper-Kurn, Superresolution Microscopy of Optical Fields Using Tweezer-Trapped Single Atoms, *Phys. Rev. Lett.* **128**, 083201 (2022).
- [50] E. Deist, Y. H. Lu, J. Ho, M. K. Pasha, J. Zeiher, Z. Yan, and D. M. Stamper-Kurn, Mid-Circuit Cavity Measurement in a Neutral Atom Array, *Phys. Rev. Lett.* **129**, 203602 (2022).
- [51] E. Uruñuela, M. Ammenwerth, P. Malik, L. Ahlheit, H. Pfeifer, W. Alt, and D. Meschede, Raman imaging of atoms inside a high-bandwidth cavity, *Phys. Rev. A* **105**, 043321 (2022).
- [52] S. Begley, M. Vogt, G. K. Gulati, H. Takahashi, and M. Keller, Optimized Multi-Ion Cavity Coupling, *Phys. Rev. Lett.* **116**, 223001 (2016).
- [53] See Supplemental Material at <http://link.aps.org/supplemental/10.1103/PhysRevLett.130.173601>, for the details of the theory of the vacuum Rabi spectra of multiatom cavity QED, the double MOT system, the scheme of the cavity locking, analysis of the consistency of the optical tweezers, the experimental sequences, and the estimation of experimental data, which includes Refs. [1,54–57].
- [54] A. Dombi, A. Vukics, and P. Domokos, Optical bistability in strong-coupling cavity QED with a few atoms, *J. Phys. B* **46**, 224010 (2013).
- [55] H. Carmichael, *An Open Systems Approach to Quantum Optics* (Springer-Verlag, New York, 1991).
- [56] M. Endres, H. Bernien, A. Keesling, H. Levine, E. Anschuetz, K. A., C. Senko, V. Vuletic, M. Greiner, and M. Lukin, Atom-by-atom assembly of defect-free one-dimensional cold atom arrays, *Science* **354**, 1024 (2016).
- [57] E. D. Black, An introduction to Pound-Drever-Hall laser frequency stabilization, *Am. J. Phys.* **69**, 79 (2001).
- [58] S. Li, G. Li, W. Wu, Q. Fan, P. Yang, P. Zhang, and T. Zhang, High-numerical-aperture and long-working-distance objective for single-atom experiments, *Rev. Sci. Instrum.* **91**, 043104 (2020).
- [59] N. Schlosser, G. Reymond, and P. Grangier, Collisional Blockade in Microscopic Optical Dipole Traps, *Phys. Rev. Lett.* **89**, 023005 (2002).
- [60] Y. O. Dudin, L. Li, F. Bariani, and A. Kuzmich, Observation of coherent many-body Rabi oscillations, *Nat. Phys.* **8**, 790 (2012).
- [61] H. Labuhn, D. Barredo, S. Ravets, S. de Leseleuc, T. Macri, T. Lahaye, and A. Browaeys, Tunable two-dimensional arrays of single Rydberg atoms for realizing quantum Ising models, *Nature (London)* **534**, 667 (2016).

- [62] Z. Wang, H. Li, W. Feng, X. Song, C. Song, W. Liu, Q. Guo, X. Zhang, H. Dong, D. Zheng, H. Wang, and D.-W. Wang, Controllable Switching between Superradiant and Subradiant States in a 10-Qubit Superconducting Circuit, *Phys. Rev. Lett.* **124**, 013601 (2020).
- [63] A. A. Kaufman, Photons and qubits get a better connection, *Science* **373**, 1436 (2021).
- [64] X. F. Zhang, Q. Sun, Y. C. Wen, W. M. Liu, S. Eggert, and A. C. Ji, Rydberg Polaritons in a Cavity: A Superradiant Solid, *Phys. Rev. Lett.* **110**, 090402 (2013).